established at relatively shallow levels comparable to the pressures in the present experiments.

Using the experimental partition coefficients, we can estimate the noble gas contents in the core: for example, $^{20}\text{Ne} < 3.7 \times 10^{-12}$ cm^3 STP/g, which is much less than the estimated amount of neon (1.01×10^{-8} cm^3 STP/g) in the mantle (*15*). Hence, we conclude that, if core separation took place under equilibrium conditions, the core contains only negligible amounts of noble gases. However, if the core contains measurable amounts of noble gases, core separation must have proceeded either under conditions quite different from the above core formation scenario, such as nonequilibrium partitioning, or under an extremely dense primitive atmosphere.

REFERENCES AND NOTES

1. M. Ozima and F. A. Podosek, *Noble Gas Geochemistry* (Cambridge Univ. Press, Cambridge, 1983)
2. H. Craig *et al.*, *Earth Planet. Sci Lett.* **26**, 125 (1975).
3. H. Craig and J. E. Lupton, *ibid.* **31**, 369 (1976).
4. G. F. Davies, *ibid.* **99**, 94 (1990)
5. D. J. Stevenson, *Lunar Planet. Sci.* **16**, 821 (1985)
6. J. Matsuda *et al.*, *Geochim. Cosmochim. Acta* **53**, 3025 (1989).
7. The diffusion data for noble gases in silicate melt were recorded at about 1500°C [from figure 5 in M. R Carroll, *Earth Planet. Sci. Lett.* **103**, 156 (1991)].
8. W G. Wolfer *et al.*, *Acta Metall.* **37**, 579 (1989).
9. H H Uhlig, *J. Phys. Chem.* **41**, 1215 (1937); M. Blander *et al.*, *ibid* **63**, 1164 (1959).
10. T Murase and A. R. McBirney, *Geol. Soc. Am. Bull.* **84**, 3563 (1973).
11. *CRC Handbook of Chemistry and Physics* (CRC Press, Boca Raton, FL, ed. 2, 1991–1992), pp 4-135–4-136
12. O. K. Rice, *J. Chem. Phys.* **15**, 333 (1947).
13. S. Hara, personal communication.
14. S. Sasaki and K. Nakazawa, *J. Geophys. Res* **91**, 9231 (1986).
15. The amount in air divided by the mass of the Earth [from (*1*)].

3 August 1992; accepted 20 November 1992

Evidence from Claw Geometry Indicating Arboreal Habits of *Archaeopteryx*

Alan Feduccia

The Late Jurassic *Archaeopteryx* has been thought to have been a feathered predator adapted to running that represented a terrestrial stage in the evolution of true birds from coelurosaurian dinosaurs. Examination of claw geometry, however, shows that (i) modern ground- and tree-dwelling birds can be distinguished on the basis of claw curvature, in that greater claw arcs characterize tree-dwellers and trunk-climbers, and (ii) the claws of the pes (hind foot) and manus (front hand) of *Archaeopteryx* exhibit degrees of curvature typical of perching and trunk-climbing birds, respectively. On this basis, *Archaeopteryx* appears to have been a perching bird, not a cursorial predator.

The fossil organism that has been the focus of most discussions of avian origins and the origin of flight (*1–3*) is the Late Jurassic (150 million years ago) *Archaeopteryx* found in the Solnhofen Limestone of Bavaria. There are now six well-preserved specimens that have been found (*4*). Two major theories for the evolution of avian flight—the cursorial theory, in which flight evolved from the ground up, and the arboreal theory, in which flight evolved from the trees down—are based on interpretations of the paleobiology and behavior of this primal bird. The genus *Archaeopteryx* has been envisioned in many ways: as an earthbound, cursorial predator that evolved feathers as insect traps (*5*), which would be a terrestrial stage in the evolution of avian flight (*6*); as a wader that used its wings, as do some modern herons and storks, to shade the water, which would aid in the capture of prey (*7*); and as a cliff clinger and climber (*8*). One hypothesis is that hot-blooded dinosaurs were clothed with feathers for insulation and were therefore preadapted for flight, an example of "exaptation" (*9*). Because claws may be an important indicator of avian habits, in this report I present data on claw geometry that are used to evaluate the habits of *Archaeopteryx*; and I discuss other morphological evidence to help define its behavior and paleobiological role in Late Jurassic ecosystems.

To determine if the geometry of the claws of the pes is a useful index for arboreal versus terrestrial habits in birds, I examined more than 500 species of birds, photographed approximately 400 claws (digit III), and traced and measured the claw arcs (*10*). These measurements were of the central angle formed by radii from the ends of the claw (Fig. 1) and represented the amount of a circle in a claw arc (*10*). Ten species each were chosen among ground-dwelling birds (five orders, seven families, ten genera), perching birds (four orders, eight families, ten genera), and trunk-climbing birds (three orders, five families, ten genera) (*11*). Birds with unusual adaptations—such as raptors, long-legged marsh birds, long-legged birds (for example, seriamas) that roost and nest low in bushes or trees, birds that resemble *Archaeopteryx*, and so forth—were avoided to eliminate as much as possible birds with claws adapted for strange habits or perceived to be generally convergent with those of *Archaeopteryx* for whatever reason.

The major separation of birds on the basis of claw arc measurements is between ground-dwellers and all others (Fig. 2). The mean for the ground-dwellers (*n* = 98) was 64.3°, and the means of individual species ranged from 52.2° to 77.6°; perching birds (*n* = 94), the closer of the other two groups, had a mean of 116.3°, and their individual means ranged from 101.8° to 125.3°. Of all ground-dwelling birds analyzed, only one individual, a *Neomorphus*, had a greater claw arc than that of a perching bird, a *Cyanocitta*.

Perching birds and trunk-climbers were for the most part separable; 100 trunk-climbers had a mean of 148.7° and means for species ranged from 129.5° to 161.6°. There was, however, some overlap of individual measurements. Some climbing species with lesser claw arc measurements, *Sitta*, *Phoeniculus*, *Certhia*, and *Trichodroma*, overlapped with some individual perchers; but only a few woodpeckers (Picidae) overlapped with the few individual perchers

Department of Biology, University of North Carolina, Chapel Hill, NC 27599.

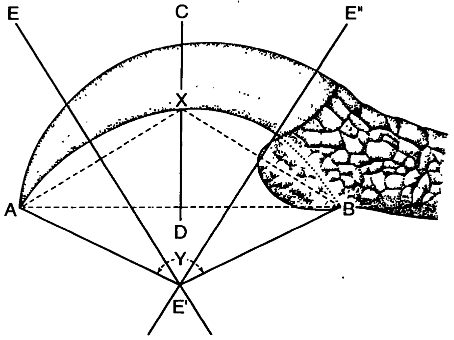

Fig. 1. Diagram of geometric measurements of claw curvature (*10*). A perpendicular (CD) is drawn to bisect the chord (AB) of the inner arc, which is itself bisected at the point X. Perpendiculars are drawn (EE' and E'E") to bisect the chords AX and XB. These perpendiculars, when extended, meet at the center (E') of the circle of which the arc is a part. The radii are then drawn to each end of the arc (AE' and BE'). The angle (Y) between these radii (read directly from a protractor) is a measure of the degrees of arc.

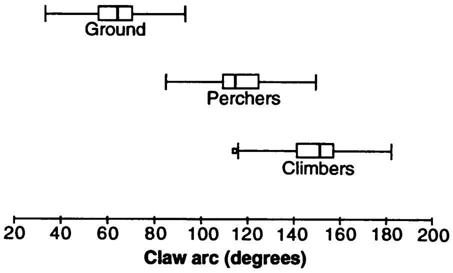

Fig. 2. Box and whiskers plot of claw arc measurements for the ten species each of ground-dwellers, perchers, and climbers (*11*). The left- and right-hand hinge values are at about the 25th and 75th percentiles of the number of points in the data, respectively. The middle line is the median and the left and right whiskers extend to values 1.5 times the spread from the median to the edge of the Tukey box. Data points falling outside these values, the box near the left hinge of "Climbers," are outliers. A one-way analysis of variance comparing all three means was significant at $P > 0.001$.

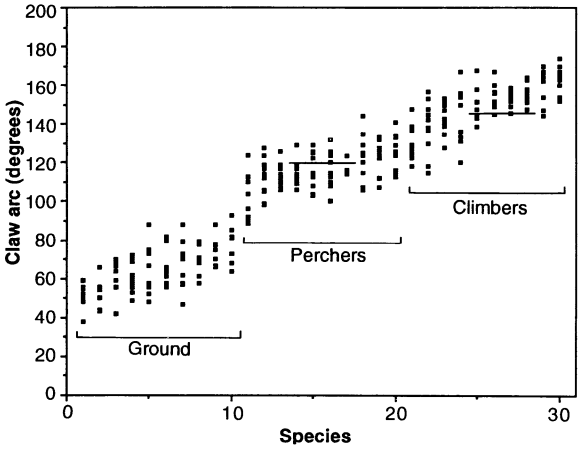

Fig. 3. Scatter diagram of the 30 species measured, in sequence from left to right as listed in (*11*), showing individual data points of claw arcs in degrees of curvature. Note the almost complete segregation of the ground-dwellers. The mean value for *Archaeopteryx* pes claws is indicated by the line in the center of perchers, and the mean for manus claws, by the line in the middle of climbers (to the right of diagram). From StatWorksTM for the Macintosh.

with the greatest arc measurements, from *Tockus* and *Pteroglossus*.

The pes claws of digit III of the measurable specimens of *Archaeopteryx* (from London, Berlin, and Eichstätt), conservatively reconstructed, are 125°, 120°, and 115°, respectively (mean of composite measurements is 120.0°); the range is 10°, well within the range for the 30 living species measured, which showed an average range of 27.1° (*11*). The Early Cretaceous, fully volant perching bird *Sinornis santensis* (6), which is only slightly younger than *Archaeopteryx*, has strongly curved claws: The curvature of its digit III claw is about 130° to 135°, which is at the upper end of perching birds, and the morphology and curvature of its digits are similar to those of recent birds within the trunk-foraging Sittidae. All of the measurements of the claws of the pes of *Archaeopteryx* fall within the range of the three strongest perching birds measured (Fig. 3), namely *Pteroglossus*, *Tockus*, and *Cuculus*. The strongly curved pes claws of *Archaeopteryx* (Fig. 4A) may have been an adaptive compensation for overall weak perching ability.

The curvatures of the middle claws of the manus of the measurable *Archaeopteryx* fossils (from Tyler, Berlin, and Solnhofen) are 155°, 142°, and 145°, respectively (mean of composite measurements is 147.3°), with a range of 18°. The manus claws (Fig. 4B) fall within the upper range of the claws of the strongest perching birds and completely within the range of claws of trunk-climbers (Fig. 3).

In overall proportions and body form, *Archaeopteryx* is similar to such modern birds as the touracos (Musophagiformes: Musophagidae), the chachalacas (Galliformes: Cracidae), and the large cuckoos of the genus *Centropus* (Cuculiformes: Centropinae) (*12, 13*). Touracos are strong perching birds, and the species that I measured, *Tauraco porphyreolophus* (n = 10), had a mean claw arc of 120.9° (range 96° to 145°, SD = 13.9). Chachalacas are both terrestrial and arboreal (*14*); *Ortalis poliocephala* (n = 10), which is more terrestrial than arboreal, had a mean claw arc of 91.0° (range 71° to 116°, SD = 16.0), whereas *Penelope argyrotis* (n = 10), which is more arboreal than terrestrial, had an almost identical claw arc of 92.9° (range 71° to 107°, SD = 9.8). This observation confirms that claw geometry of birds that are both tree- and ground-dwellers (for example, grackles, *Quiscalus*; crows, *Corvus*; hoopoes, *Upupa*; and ground pigeons, *Goura*) tends to reflect the terrestrial more than the arboreal adaptation. One exception is flickers (*Colaptes*), which have strongly curved claws; these normally arboreal birds do climb walls, and some nest in cliffs high in the Andes. On the other hand, the only true ground woodpecker, *Geocolaptes olivaceus* (n = 3), had claw arc measurements of 84°, 95°, and 98°, still in the upper end of the true ground-dwellers. The pheasant cuckoo or swamp pheasant of Australia, *Centropus phasianinus*, has a morphological profile that is almost identical to that of *Archaeopteryx* (Fig. 5), except that its tail and body feathers are loosely constructed and its wing is less elliptical (both characteristic of terrestrial birds in general). Its claw arc (n = 10), however, averages 85.7° (range 65° to 101°, SD = 10.2), well within the range of ground-dwellers and outside the range of perching birds and *Archaeopteryx*.

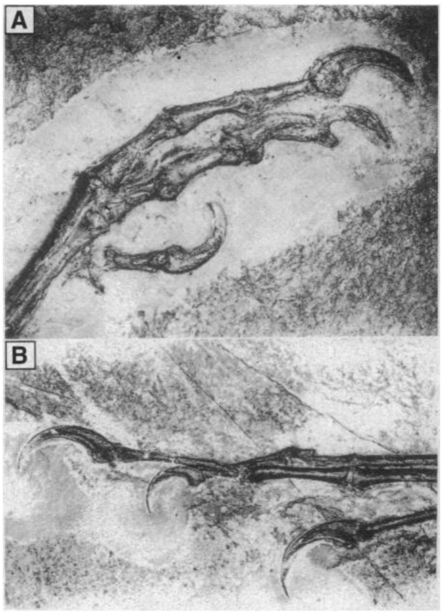

Fig. 4. (**A**) Medial view of the left pes of the London specimen (British Museum of Natural History) of *Archaeopteryx*, which shows the claw curvature typical of strong perching birds. (**B**) Dorsal view of the right manus of the Berlin specimen, which shows the manus claws which are closest in morphology to those of modern trunk-climbing woodcreepers (Passeriformes: Dendrocolaptidae).

Yalden (*15*) discovered that the claws of the manus of *Archaeopteryx* are very similar to those of trunk-climbing birds and mammals and suggested that *Archaeopteryx* used the manus claws in trunk-climbing. Morphologically, the manus claws are almost identical to pes claws of neotropical trunk-climbing woodcreepers (Dendrocolaptidae), specifically *Xiphocolaptes* and *Hylexetastes*. The claws of a clinging bird, namely, the swift [*Streptoprocne zonaris* (n = 10)], while morphologically different from those of the manus of *Archaeopteryx*, had a mean of 131.9° (range 122° to 138°, SD = 6.4); half of the individuals measured had claw arc measurements that overlapped the manus claw measurements of *Archaeopteryx*. Manus claws of *Archaeopteryx* also agree in morphology with those of tree-trunk–climbing or –clinging mammals such as *Cynocephalus*, *Pteropus*, *Hipposideros*, *Sciurus*, *Schoinobates*, and *Petaurus* [see also (*15*)]. Based on these observations and

Fig. 5. Silhouette of *Archaeopteryx* (right) compared with that of its "look-alike," the Australian pheasant cuckoo, *Centropus phasianinus* (left); these show remarkable superficial morphological similarity (*12, 13*). *Centropus* differs in that it is predominantly terrestrial. It therefore, unlike *Archaeopteryx*, possesses a loosely constructed tail, normally exhibiting fraying at the tip, and a loosely constructed wing, showing less ellipticity. Its claw-arc measurements give a mean of 85.7° (n = 10), typical of ground-dwellers. [Adapted from (*12*)]

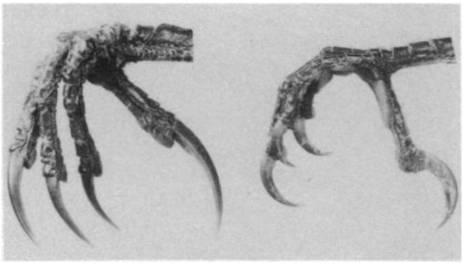

Fig. 6. External morphology of the foot of (left) the lyrebird (*Menura novaehollandiae*: Menuridae), a predominantly ground-dwelling bird, which shows the distinctive straight claws of a ground-dweller; compared with (right) the foot of a bowerbird (*Chlamydera nuchalis*: Ptilonorhynchidae), which are like those of the *Archaeopteryx* and have the curved claws of a perching bird. Not to scale.

comparisons of the manus claws of *Archaeopteryx* with those of woodpeckers, Yalden (*15*) concluded that *Archaeopteryx* was a trunk-climber.

Manus claws of *Archaeopteryx* differ markedly from those of predatory dinosaurs in that they exhibit lateral compression in extensor view and have needlelike points. The claws of predators, including theropods, tend to be conical and smoothly tapered (*15*). Predatory birds have wide pes claws with lateral cutting edges. Pes claws of theropods (for example, *Compsognathus*) are characterized by small arc angles, like those of ground-dwelling birds.

One can infer from the claw-arc measurements of the pes of *Archaeopteryx* that it was a perching bird (Fig. 6). Many types of arborescent plants found in the lagoonal deposits of Solnhofen and Nusplingen during the Late Jurassic [including numerous seed ferns (pteridosperms), conifers (coniferopsids), Bennettitales (*Zamites*), and ginkgos (*16*)] could have provided a suitable place to perch.

The claws of the *Archaeopteryx* manus, however, are more difficult to interpret (*8*), primarily because the claws of the pes are not, as those of the manus appear to be, those of a strongly adapted trunk-climber. Most likely, *Archaeopteryx* used the claws of the manus for clinging to branches because it had not yet achieved the balance that is characteristic of modern birds (*17, 18*). It was capable of trunk-climbing but may have done so only occasionally, after flying to the ground. *Archaeopteryx* was probably incapable of taking off from the ground (*19*); climbing would have allowed the bird to reach a suitable place from which to launch, where it could take advantage of the cheap energy provided by gravity.

Other evidence suggests that *Archaeopteryx* had an advanced aerodynamic morphology (*20*). (i) It had the feathers of modern birds, unchanged in structural detail over 150 million years of evolution, including microstructure, like regular spacing of barbs throughout the feather's length and clear impressions of barbules (*18, 21*). (ii) The vanes of its flight feathers were asymmetric, producing individual airfoils (*22*), as in modern volant birds; the remiges, specialized flight feathers, of secondarily flightless birds revert to symmetry (*22*). (iii) The remiges of *Archaeopteryx* were curved, an expression of aerodynamic design seen in modern volant birds (*23*). (iv) Its flight feathers had a ventral, reinforcing furrow, as in modern flying birds (*21*). (v) *Archaeopteryx* exhibited the classic elliptical wing of modern woodland birds. This wing design is very efficient at low to moderate speeds and is present in modern passerines, galliforms, piciforms, columbiforms, and even the woodcock (*24*). (vi) *Archaeopteryx* also exhibited a hypertrophied furcula (fused clavicles), which provided an expanded site of attachment for the pectoral muscles, which effect the downstroke of the wing (*19*). (vii) Its scapula met the coracoid at an angle of approximately 90°, a condition characteristic of only modern volant birds. This adaptation reduces the distance that the dorsal elevators of the wing must act to effect the recovery stroke (*19, 20*). The validity of this observation would be reinforced if, as thought, *Archaeopteryx* lacked a keeled sternum. (viii) Its tail was designed to provide lift in flight (*25*) and was not loosely constructed; nor did it show signs of fraying, which is characteristic of terrestrial birds (*12, 13*). (ix) Finally, *Archaeopteryx* had a fully reversed hallux, the large rear toe (*17, 18*), with a strongly curved claw on the ungual phalanx, which is typical of modern perching birds and unlike any known theropod dinosaur.

In consideration of the above morphological features, flight adaptations that represent shared, derived characters (synapomorphies) with modern volant birds, I conclude that *Archaeopteryx* was arboreal and volant, considerably advanced aerodynamically, and probably capable of flapping, powered flight to at least some degree (*20*). *Archaeopteryx* probably cannot tell us much about the early origins of feathers and flight in true protobirds because *Archaeopteryx* was, in the modern sense, a bird.

REFERENCES AND NOTES

1. W. J. Bock, in *The Origin of Birds and the Evolution of Flight*, K. Padian, Ed. (Memoir 8, California Academy of Sciences, San Francisco, 1986), pp. 57–72.
2. L. M. Witmer, in *Origins of the Higher Groups of Tetrapods*, H.-P. Schultze and L. Trueb, Eds. (Cornell Univ. Press, Ithaca, NY, 1991), pp. 427–466.
3. J. M. Rayner, in *Biomechanics in Evolution*, J. M. Rayner and R. J. Wootton, Eds. (Cambridge Univ. Press, Cambridge, 1991), pp. 183–212.
4. P. Wellnhofer, *Science* **240**, 1790 (1988).
5. J. H. Ostrom, *Q. Rev. Biol.* **49**, 1 (1976); *Am. Sci.* **67**, 46 (1979); in (*2*), pp. 467–484.
6. P. C. Sereno and R. Chenggang, *Science* **255**, 845 (1992).
7. R. A. Thulborn and T. L. Hamley, in *The Beginnings of Birds*, M. K. Hecht, J. H. Ostrom, G. Viohl, P. Wellnhofer, Eds. (Freunde des Jura-Museums, Eichstätt, Germany, 1985), pp. 81–89.
8. D. S. Peters and E. Görgner, *Sci. Ser.* (*Los Angeles*) **36**, 29 (1992).
9. S. J. Gould and E. Vrba, *Paleobiology* **8**, 4 (1982).
10. The claw of digit III was photographed with the use of a macrofocusing lens. Slides were projected so that claws could be traced at a size of 10 to 15 cm; a line, traced from the claw tip to the base of the ungual phalanx, approximated a true arc and was measured as such. This is a modification of a similar technique used by W. L. Engles [*Univ. Calif. Publ. Zool.* **42**, 341 (1940)] to study bill arcs and modified by F. Richardson [*ibid.* **46**, 317 (1942)] to study claw arcs of tree-trunk–foraging birds. This approach has an advantage over other indirect methods (*8*) in that the measurement is more easily realizable physically. Large angles are indicative of curved claws and an arboreal habit; small angles imply flat claws and a ground-dwelling habit.
11. Ten species each were chosen among ground-dwellers, perching birds, and trunk-climbing birds. Where possible, a sample of ten specimens of each species was used. The following species were measured (listed from smallest to largest claw-arc angle): Ground-dwellers: *Eudromia elegans* (n = 10, for all unless indicated) (mean 60.5, range 42 to 70, SD 5.5; all data points are available upon request), *Apteryx australis* (n = 6) (52.2, 43 to 66, 7.8), *Gallus varius* (60.5, 42 to 70, 7.6), *Colinus virginianus* (n = 12) (61.0, 53 to 72, 6.7), *Gallirallus australis* (64.0, 48 to 88, 11.7), *Geococcyx californiana* (65.6, 56 to 82, 8.3), *Numida meleagrides* (66.8, 47 to 88, 11.3), *Geositta cunicularia* (70.2, 58 to 79, 6.8), *Sturnella magna* (70.9, 66 to 88, 7.0), and *Neomorphus geoffroyi* (77.6, 64 to 93, 8.6). Perching birds: *Cyanocitta cristata* (101.8, 89 to 124, 10.8), *Myiarchus crinitus* (112.2, 98 to 128, 9.6), *Coracias benghalensis* (113.3, 106 to 126, 5.7), *Ramphococcyx calyorhynchus* (113.8, 106 to 129, 6.1), *Coccyzus americanus* (115.9, 103 to 129, 8.8), *Momotus momota* (116.2, 100 to 132, 8.97), *Leptosomus discolor* (n = 3) (118, 114 to 124, 4.32), *Pteroglossus frantzii* (122.9, 106 to 144, 11.2), *Cuculus sparverioides* (124.1, 107 to 133, 8.2), and *Tockus fasciatus* (125.3, 113 to 141, 9.1). Trunk-climbing birds: *Sitta carolinensis* (129.5, 118 to 148, 8.7), *Phoeniculus purpureus* (138.3, 115 to 157, 13.2), *Certhia americana* (142.9, 128 to 153, 7.5), *Trichodroma muraria* (141.1, 120 to

167, 13.9), *Sphyrapicus varius* (149.0, 139 to 168, 8.2), *Xiphorhynchus guttatus* (153.7, 145 to 160, 6.1), *Picoides villosus* (154.4, 146 to 159, 4.1), *Campethera caroli* (156.4, 148 to 164, 5.4), *Picus canus* (160.9, 144 to 170, 8.9), and *Dryocopus pileatus* (161.1, 152 to 174, 7.5).
12. O. Heinroth, *J. Ornithol.* **71**, 277 (1923).
13. P. Brodkorb, in *Avian Biology*, D. S. Farner and J. R. King, Eds. (Academic Press, New York, 1971), vol. 1, pp. 19–54.
14. J. Delacour and D. Amadon, *Currassows and Related Birds* (American Museum of Natural History, New York, 1973).
15. D. W. Yalden, in (*7*), pp. 91–97.
16. O. Mutschler, *Jahresber. Mitt. Oberrheinischen Geol. Ver.* **16**, 25 (1927); K. W. Barthel, N. H. M. Swinburne, S C. Morris, *Solnhofen· A Study in Mesozoic Paleontology* (Cambridge Univ. Press, Cambridge, 1990).
17. S. Tarsitano, in (*7*), pp. 319–332.
18. L. D. Martin, in (*2*), pp. 485–540.
19. M. Sy, *J Ornithol.* **84**, 199 (1936); S. L Olson and A. Feduccia, *Nature* **278**, 247 (1979).
20. A. Feduccia, *The Age of Birds* (Harvard Univ Press, Cambridge, MA, 1980), U. M Norberg, *Vertebrate Flight* (Springer-Verlag, Berlin, 1990)
21. S. Rietschel, in (*7*), pp 251–260.
22. A. Feduccia and H. B. Tordoff, *Science* **203**, 1021 (1979)
23. R. Å. Norberg, in (*7*), pp. 308–318
24. D B. O. Savile, *Evolution* **11**, 212 (1957).
25. D W. Yalden, *Nature* **231**, 127 (1971); *Ibis* **113**, 349 (1971).
26. I thank V. Albert, W. Bock, L. Martin, S. Olson, and S Tarsitano for comments on the manuscript and W. Dickison, P. Gensel, and M Urlichs for paleobotanical advice. V. Albert helped with statistics and Figs. 2 and 3 and S. Tarsitano provided photos for Fig 4. S. Olson provided access to the collections of the U.S National Museum of Natural History. S Whitfield prepared Figs. 1, 5, and 6

11 September 1992; accepted 15 December 1992

A High-Temperature Superconducting Receiver for Nuclear Magnetic Resonance Microscopy

R. D. Black, T. A. Early, P. B. Roemer, O. M. Mueller,
A. Mogro-Campero, L. G. Turner, G. A. Johnson

A high-temperature superconducting-receiver system for use in nuclear magnetic resonance (NMR) microscopy is described. The scaling behavior of sources of sample and receiver-coil noise is analyzed, and it is demonstrated that Johnson, or thermal, noise in the receiver coil is the factor that limits resolution. The behavior of superconductors in the environment of an NMR experiment is examined, and a prototypical system for imaging biological specimens is discussed. Preliminary spin-echo images are shown, and the ultimate limits of the signal-to-noise ratio of the probe are investigated.

In high-field (>0.5 T) clinical magnetic-resonance imaging, the patient's body is the main source of experimental noise (*1*) that degrades image quality. As the dimensions of an imaging experiment are reduced (that is, both the specimen and coil are reduced in size), there is a crossover point beyond which the noise of the receiving coil and its associated electronics dominates. The point at which this crossover occurs depends on the strength of the applied magnetic field and on the nuclear spin density of the specimen (*2*). When the specimen no longer dominates the signal-to-noise ratio (SNR) it makes sense to reduce the receiver coil noise, which is thermal (Johnson) noise (*3*), to improve image resolution and reduce data acquisition time (*4*). The Johnson noise power is proportional to the product of resistance and temperature; therefore, reductions in these parameters will have the desired effect. Superconducting materials are clearly attractive candidates for this purpose. This report addresses the details of constructing an NMR imaging probe that incorporates the high-temperature superconductor $Y_1Ba_2Cu_3O_7$ (YBCO).

Table 1 shows how SNR varies with the dimensions of the imaging experiment and with the field strength or, equivalently, the Larmor precessional frequency ω (*5*). The NMR voltage has an r^2 dependence (where r is the linear scale dimension of the sample and receiver coil) owing to the r^3 dependence of spin number on volume and the fact that coil sensitivity goes as r^{-1}. The Bloch equations (*6*) show the origin of the ω^2 dependence. The noise power of the sample is proportional to ω^2 (*7*) and to volume, so the noise voltage of the sample goes as $(\omega^2 r^3)^{1/2}$. The Johnson noise power of the coil is proportional to the resistance R, which is, in turn, proportional to the inverse of the skin depth: skin depth goes as $\omega^{-1/2}$. Therefore, coil noise voltage goes as $\omega^{1/4}$. There is no change in resistance with scaling in the skin depth limit.

To get a physical feeling for the scaling laws, consider a typical experiment at 1.5 T that acquires an image of the human head (*1*). The sample noise power is about ten times that of the coil noise (we neglect noise contributions from the cabling and preamplifier). Shrinking the scale dimension by a factor of ~2 would make the noise powers about equal. If the diameter of the coil around the head is 25 cm, then the coil size at which the noise terms cross is about 12 cm (at 7 T, the scale dimension at which the noise powers become comparable is about 5 cm). Alternatively, if the human head coil stays the same size, the sample and coil noise terms will be comparable when the field is reduced from 1.5 to 0.3 T. It is clear that superconducting head coils designed to work at 1.5 T would not be useful because the patient noise dominates. However, for sample sizes in the range of 1 cm or less in a field of 7 T, a big improvement in SNR can be achieved if we reduce the coil noise.

Two principal issues complicate the use of superconducting materials in NMR imaging. Superconductors revert to the normal, nonsuperconducting state in sufficiently high magnetic fields and at large enough temperatures. None of the elemental superconductors (such as Nb or Pb) can withstand the 7-T field or the 10 K operating temperature that exists in the system described below. The A-15 materials (for example, Nb_3Sn and Nb_3Al) have critical parameter values that are large enough, but tests of the Nb_3Al film resonators that we constructed showed them to have lower quality factors than the YBCO film resonators that we made. The extremely high critical temperature and the critical field values of YBCO films make them the best choice.

The YBCO films were produced by coevaporation and post-annealing procedures that are described elsewhere (*8*). The 0.6-μm-thick films were deposited onto both sides of a 0.5-mm-thick, 2.5-cm-diameter $LaAlO_3$ substrate. We chose $LaAlO_3$ for its crystallographic compatibility with YBCO and its relatively low dielectric loss tangent. The films were patterned with the use of conventional photolithographic techniques and were etched with 0.01 N nitric acid. The YBCO was patterned into a split ring shape (18-mm outer and 14-mm inner di-

Table 1. Scaling laws for NMR imaging. The frequency ω is proportional to magnetic field strength. The linear scale size of the sample and coil is represented by r. One can determine the constant A empirically by measuring the sample and coil losses for head images at 1.5 T. When the coil is cooled, its voltage noise will decrease by a factor equal to the square root of the ratio of the coil temperature to the sample temperature. SNR is signal-to-noise ratio.

NMR voltage	$\omega^2 r^2$
Sample noise voltage	$\omega r^{3/2}$
Coil noise voltage	$\omega^{1/4}$
Intrinsic SNR (sample)	$\omega r^{1/2}$
SNR (coil + sample)	$\dfrac{\omega^2 r^2}{\sqrt{\omega^2 r^3 + A\omega^{1/2}}}$
Imaging time	$1/(\mathrm{SNR})^2$

R. D Black, T. A. Early, P B. Roemer, O M. Mueller, A. Mogro-Campero, L. G Turner, General Electric Corporate Research and Development Center, Schenectady, NY 12301.
G. A. Johnson, Departments of Radiology and Physics, Duke University, Durham, NC 27710.